Homozygous Rare *PARN* Missense Mutation in Familial Pulmonary Fibrosis

To the Editor:

Idiopathic pulmonary fibrosis (IPF) is a devastating disease with a life expectancy of 3–5 years that usually affects individuals older than 50 years of age (1, 2). Both the familial and sporadic forms of adult-onset pulmonary fibrosis are linked to heterozygous rare variants of telomere-related genes (3), including *PARN*, a polyadenylation-specific RNase essential for maturation of telomerase RNA (4). Diallelic or homozygous rare variants in *PARN* have been found in children with dyskeratosis congenita and Hoyeraal–Hreidarsson syndromes (5). This is the first report of three siblings affected with adult-onset familial pulmonary fibrosis who are homozygous for a rare *PARN* mutation, which has a 7.4-fold higher frequency in individuals of Hispanic ethnicity.

Patients

This study was approved by the institutional review board at the University of Texas Southwestern Medical Center. Written consent was obtained from all subjects.

The proband (II.4; Figure 1) was a marathon runner before his diagnosis of IPF was made at age 60 years by computed tomography imaging of the chest and transbronchial biopsy of the lung. His lung function rapidly deteriorated (FVC 29% predicted and D_{LCO} 10% predicted). He underwent bilateral lung transplantation at age 61 years and has had few complications for >3 years besides mild thrombocytopenia and red blood cell macrocytosis. His older brother (II.3) was diagnosed with IPF after surgical lung biopsy at age 51 years. His lung function was stable until age 55 years. He developed rapidly progressive hypoxemia and died while being listed for lung transplantation. He did not have any cytopenias. His younger sister (II.5) had a history of primary biliary cirrhosis and was diagnosed with pulmonary fibrosis by high-resolution computed tomography (non–usual interstitial pneumonia pattern) at age 53 years. Transbronchial lung biopsies were unrevealing, and laboratory studies demonstrated thrombocytopenia, red blood cell macrocytosis, positive antinuclear antibody (1:2,560, centromere pattern), and elevated sedimentation rate. She was treated with immunosuppressive medications for a presumed autoimmune disease and expired from staphylococcal pneumonia at age 54 years.

Two of the affected individuals noted graying of hair before 30 years of age. By family report, the father (I.1) was diagnosed with asbestos-related lung disease and the mother (I.2) had lung disease, but medical records were not available for either.

Results

Whole-exome sequencing of the proband (II.4) was performed by the McDermott Center Sequencing Core at UT Southwestern, using the KAPA Hyper Prep Kit (Kapa Biosystems) and the xGen Exome Research Panel (Integrated DNA Technologies); paired-end 150-bp read length sequencing was obtained using NextSeq 500 (Illumina). Median on-target coverage was 97-fold, with more than 97.5% target regions having at least 20-fold coverage. Sequences were aligned to human reference genome hg19, and variants were called using Genome Analysis Toolkit and annotated using

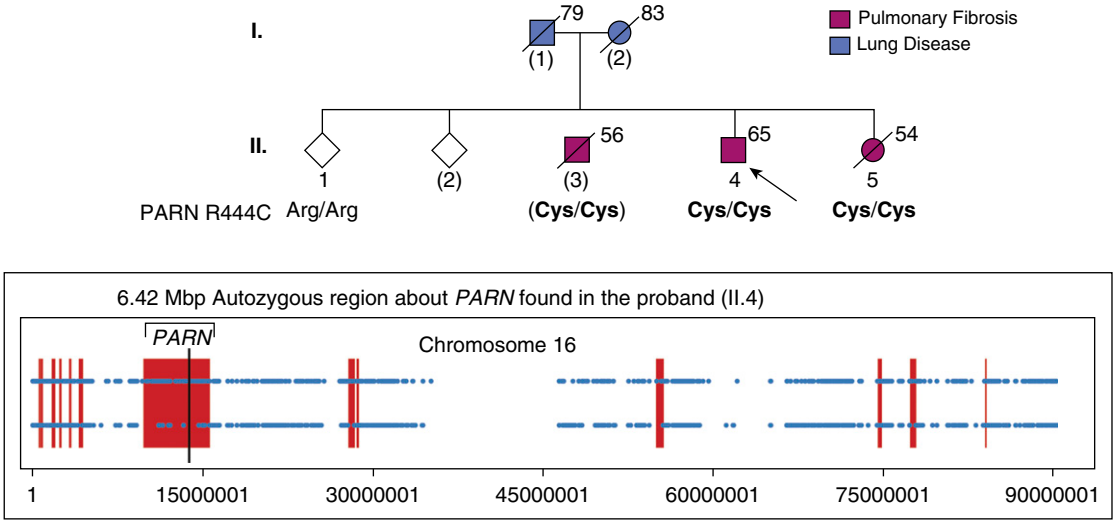

Figure 1. Phenotypic and genetic characterization of an adult-onset familial pulmonary fibrosis kindred. Individuals with pulmonary fibrosis or an unclassified lung disease are indicated by purple and blue symbols, respectively. Unfilled symbols represent individuals with no reported lung disease. The arrow indicates the proband. Numbers in parentheses indicated individuals for whom no DNA sample was available. Age in years at the time of blood draw or death is indicated to the right of each symbol. The genotypes of individual II.3 were inferred from the haplotypes of his children (data not shown). The pedigree was modified to protect the identities of the participants. Inset shows autozygous regions of chromosome 16 (red blocks) determined from the exome sequencing data of the proband (II.4).

Supported by R01HL093096 (C.K.G.) and T32HL098040 (D.Z.).

Originally Published in Press as DOI: 10.1164/rccm.201809-1632LE on December 10, 2018

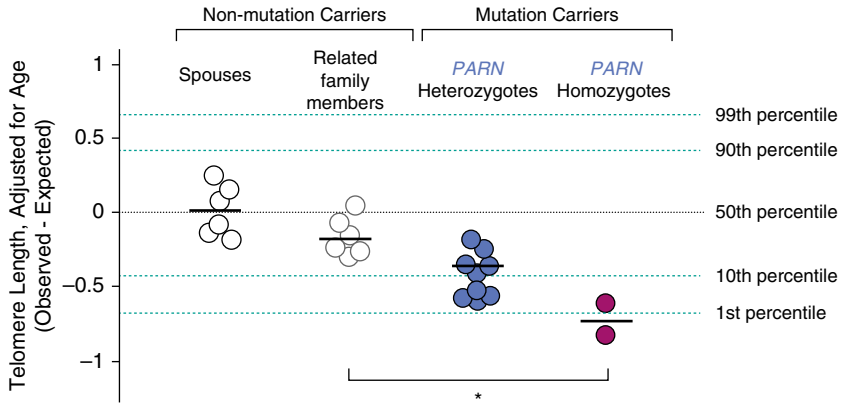

Figure 2. Dosage of *PARN* p.Arg444Cys variant associated with telomere shortening. Telomere length of genomic DNA isolated from circulating leukocytes from members of one family as measured by multiplexed quantitative PCR assay (7). Telomere lengths are adjusted for age and are expressed as the observed length minus the expected length. Each symbol represents a unique individual. White circles outlined in black represent unrelated spouses. Telomere lengths were significantly different across the three groups (zero, one, and two copies of the *PARN* allele) by one-way ANOVA (*$P = 0.0006$).

snpEff. A homozygous missense mutation in *PARN* (c.1330C>T, p.Arg444Cys) was identified in the proband. No other rare variants were found in the other genes linked to pulmonary fibrosis (*TERT*, *TERC*, *RTEL1*, *NAF1*, *DKC1*, *TINF2*, *SFTPA1/2*, and *SFTPC*). The *PARN* variant affects a highly conserved region of the RNA recognition domain. Commercial genetic sequencing of the sister (II.5) revealed the same homozygous *PARN* missense variant and was classified as a variant of uncertain significance. The frequency of this variant is ~7.4-fold higher in individuals of Latino ethnicity (Genome Aggregation Database [gnomAD] allele frequency of 0.0001756) than individuals of European (Non-Finnish) ethnicities (gnomAD allele frequency of 0.0000238). We determined the genotypes of the *PARN* allele and flanking polymorphic markers for all available family members; two distinct haplotypes containing the *PARN* Arg444Cys allele were found to segregate in the family (data not shown).

Analysis of the whole-exome sequencing data of the proband (II.8) using BCFtools (6) revealed a 6.42-megabp autozygous region encompassing the *PARN* locus (Figure 1, inset). The inbreeding coefficient for the proband was calculated to be 6.6%, suggesting that his parents (I.1 and I.2) share similar amounts of DNA as third-degree relatives. We surmise that the haplotype about *PARN* was inherited from a common ancestor. Although there is no known consanguinity of the parents, both were born of Latino ancestry and lived in a sparsely populated region.

Leukocyte telomere lengths were measured using a quantitative polymerase chain reaction assay (7) of all available family members and spouses (Figure 2). As a group, individuals homozygous for the *PARN* p.Arg444Cys variant had the shortest telomere lengths. We found significant differences in age-adjusted telomere lengths for those who had inherited zero, one, or two variant alleles. This data is compatible with a gene-dosage effect of the *PARN* variant on blood telomere lengths, consistent with its role in the biogenesis of telomerase RNA (4).

Discussion

We describe the first report of a homozygous *PARN* mutation that co-segregates with adult-onset pulmonary fibrosis. All other reported diallelic or homozygous PARN mutations have been seen in young children with dyskeratosis congenita or Hoyeraal–Hreidarsson syndrome, the oldest of which was 10 years of age (8). The onset of pulmonary fibrosis and shorter blood telomere lengths in affected individuals of this kindred are likely related to a *PARN* variant-dosage effect.

The parents of the affected individuals were both obligate heterozygotes. Their history of lung disease late in life suggests a risk for developing pulmonary illness that is lower than homozygotes but higher than individuals who do have this variant. Additional studies will be needed to determine whether this rare missense variant represents a Hispanic ethnicity–specific pulmonary fibrosis genetic risk factor. Accurate counseling of at-risk family members who inherit this *PARN* missense variant could not be provided without knowledge of the allele-dosage effect revealed by this investigation. This case highlights the complex inheritance patterns that may be associated with rare *PARN* missense alleles in adults. These findings strengthen the link between adult-onset pulmonary fibrosis and telomere attrition and implicates a homozygous rare *PARN* missense variant as the potential genetic cause. ■

Author disclosures are available with the text of this letter at www.atsjournals.org.

Acknowledgment: We are grateful to the family for their participation, to Cassandra Hamilton for help in collecting blood samples, to Ross Wilson for technical assistance and to the UT Southwestern McDermott Next Generation Sequencing and Bioinformatics Cores.

David Zhang, M.D.
Zhengyang Zhou, Ph.D.
Muhanned Abu-Hijleh, M.D.
Kiran Batra, M.D.
Chao Xing, Ph.D.
Christine Kim Garcia, M.D., Ph.D.*
University of Texas Southwestern Medical Center
Dallas, Texas

ORCID ID: 0000-0002-2983-9796 (D.Z.).

*Corresponding author (e-mail: ckg2116@cumc.columbia.edu).

References

1. Raghu G, Chen SY, Yeh WS, Maroni B, Li Q, Lee YC, *et al*. Idiopathic pulmonary fibrosis in US Medicare beneficiaries aged 65 years and older: incidence, prevalence, and survival, 2001-11. *Lancet Respir Med* 2014;2:566–572.
2. Raghu G, Collard HR, Egan JJ, Martinez FJ, Behr J, Brown KK, *et al*.; ATS/ERS/JRS/ALAT Committee on Idiopathic Pulmonary Fibrosis. An official ATS/ERS/JRS/ALAT statement: idiopathic pulmonary fibrosis. Evidence-based guidelines for diagnosis and management. *Am J Respir Crit Care Med* 2011;183:788–824.
3. Garcia CK. Insights from human genetic studies of lung and organ fibrosis. *J Clin Invest* 2018;128:36–44.
4. Moon DH, Segal M, Boyraz B, Guinan E, Hofmann I, Cahan P, *et al*. Poly(A)-specific ribonuclease (PARN) mediates 3′-end maturation of the telomerase RNA component. *Nat Genet* 2015;47:1482–1488.
5. Tummala H, Walne A, Collopy L, Cardoso S, de la Fuente J, Lawson S, *et al*. Poly(A)-specific ribonuclease deficiency impacts telomere biology and causes dyskeratosis congenita. *J Clin Invest* 2015;125: 2151–2160.
6. Narasimhan V, Danecek P, Scally A, Xue Y, Tyler-Smith C, Durbin R. BCFtools/RoH: a hidden Markov model approach for detecting autozygosity from next-generation sequencing data. *Bioinformatics* 2016;32:1749–1751.
7. Stuart BD, Lee JS, Kozlitina J, Noth I, Devine MS, Glazer CS, *et al*. Effect of telomere length on survival in patients with idiopathic pulmonary fibrosis: an observational cohort study with independent validation. *Lancet Respir Med* 2014;2:557–565.
8. Dhanraj S, Gunja SM, Deveau AP, Nissbeck M, Boonyawat B, Coombs AJ, *et al*. Bone marrow failure and developmental delay caused by mutations in poly(A)-specific ribonuclease (PARN). *J Med Genet* 2015; 52:738–748.

Enhanced Pulmonary Artery Radiodensity in Pulmonary Arterial Hypertension: A Sign of Early Calcification?

Pulmonary arterial hypertension (PAH) shares similarities with other vasculopathies involving arterial thickening, such as atherosclerosis, in which vascular calcifications are common and associated with an increased risk of mortality (1, 2). Noncontrast computed tomography (CT) has progressively been recognized as a reliable method to assess calcification and plaque burden, providing additional risk stratification information (2). More recently, a similar remodeling process was shown in PAH, with microscopic pulmonary artery (PA) calcifications being observed almost invariably in humans with end-stage PAH (3). Given the relationship between the radiodensity of systemic vessels on CT scans and calcified content in human vessels, with values of >130 Hounsfield units (HU) suggesting early calcification (4, 5), we hypothesized that enhanced PA peak wall attenuation (PA_{PWA}) would be an early phenomenon correlating with disease severity and predicting survival in PAH. This retrospective study was approved by our institutional review board (CER20773). Some of these study results have been previously reported in the form of an abstract (6).

Supported by personal funds of the investigators.

Originally Published in Press as DOI: 10.1164/rccm.201806-1027LE on December 20, 2018

Noncontrast thoracic CT scans performed within 3 months of baseline right-heart catheterization of patients with idiopathic PAH (IPAH), PAH associated with scleroderma (PAH-SSc), and pulmonary venoocclusive disease (PVOD) were retrospectively analyzed blindly by a medical student trained in cardiothoracic imaging using the Impax Agfa HealthCare imaging software. Patients were diagnosed and treated according to current guidelines and individually matched for sex, age, and scleroderma status, with subjects without PAH who had undergone a nonenhanced CT scan showing no evidence of parenchymal disease. Images were obtained at full inspiration (tube voltage 120 kVp, slice thickness 1 mm). The PA_{PWA} of visible vessels, defined as the maximal radiodensity measured within the wall of each PA visible on the CT scan, was assessed on three axial slices (1 cm above the upper margin of the aortic arch, and 1 cm below the carena and the right inferior pulmonary vein) and averaged out for each patient. Measured values of <50 HU were excluded to minimize measurement bias due to vessel content or surrounding elements (e.g., parenchyma). The maximum radiodensity of the descending aortic wall was similarly evaluated on the two lower slices.

A total of 84 patients with PAH (IPAH [$n = 32$], PAH-SSc [$n = 31$], and PVOD [$n = 21$]; age 63 ± 11 yr, 6-min-walk distance [6MWD] 304 ± 120 m, mean PA pressure 44 ± 13 mm Hg, pulmonary vascular resistance 690 ± 391 dyn · s/cm^5) were included in the study. PA_{PWA} was significantly increased in patients with PAH compared with control subjects (176 ± 71 vs. 118 ± 52 HU, $P < 0.0001$), as well as within each PAH subgroup (Figure 1). Among patients with PAH, PA_{PWA} did not correlate with age ($r = 0.056$, $P = 0.614$), symptom duration ($r = 0.325$, $P = 0.140$), 6MWD ($r = -0.065$, $P = 0.447$), cardiac index ($r = -0.048$, $P = 0.652$), right atrial pressure ($r = 0.044$, $P = 0.721$), mean PA pressure ($r = 0.214$, $P = 0.050$), or estimated PA compliance ($r = -0.167$, $P = 0.136$). However, PA_{PWA} correlated with pulmonary vascular resistance ($r = 0.239$, $P = 0.033$) and aortic wall attenuation ($r = 0.316$, $P = 0.003$). Aortic wall attenuation also correlated with age in patients with PAH ($r = 0.437$, $P < 0.0001$) and control subjects ($r = 0.449$, $P < 0.0001$), as previously reported (6).

During a mean follow-up of 32 ± 33 months, 54 patients (64%) died or were transplanted (Figure 2). In a univariate analysis, baseline PA_{PWA} correlated with transplant-free survival (hazard ratio [HR], 1.06 per 10 HU; 95% confidence interval [CI], 1.02–1.10; $P = 0.002$). In a multivariate analysis that also incorporated PAH type, World Health Organization functional class, cardiac index, and pulmonary vascular resistance, only PA_{PWA} (HR, 1.07 per 10 HU; 95% CI, 1.03–1.13; $P = 0.002$) and 6MWD (HR, 0.994/m; 95% CI, 0.991–0.997; $P < 0.001$) correlated with survival.

This study demonstrated that in addition to enlarged proximal PA and vascular pruning of the distal vessels, PAH was also characterized by greater PA_{PWA} on nonenhanced CT scans. Moreover, mean PA_{PWA} was increased in all PAH subtypes, and this observation could not be explained by differences in hematologic parameters or aortic radiodensity (7). Although PA_{PWA} was poorly correlated with traditional markers of disease severity in PAH, it may predict long-term outcomes.

Vascular calcification was recognized as early as the 19th century and was documented as a risk factor for cardiovascular events. The advent of the CT scan has allowed objective assessment of major vessel calcifications. It has been progressively recognized as